1   *Electronic Supplementary Information*

2   Novel optoelectronic metal organic framework material perylene

3   tetracarboxylate magnesium: preparation and biosensing

4   Fangjing Mo, Qian Han, Min Chen, Hui Meng, Jiang Guo, Yingzi Fu*

5 *Key Laboratory of Luminescence Analysis and Molecular Sensing (Southwest*

6 *University), Ministry of Education, School of Chemistry and Chemical Engineering,*

7 *Southwest University, Chongqing 400715, China.*

8

9   *Corresponding author: Tel: +86-023-68252277, E-mail address: <u>fyzc@swu.edu.cn</u>
10

Table of Contents

1. Materials and reagents

tetrabutylammonium hexafluorophosphate (TBAPF$_6$), N-hydroxy succinimide (NHS) and N-(3-dimethylaminopropyl)-N-ethylcarbodiimide hydrochloride (EDC) were purchased from J&K Chemical Co. (Beijing, China). Ferrocene (Fc), dimethylamine borane (DMAB) and nitric acid (HNO$_3$) were bought from Shanghai Macklin Biochemical Co., Ltd. Aminated zinc oxide nanoparticles (ZnO NPs), *N,N*-dimethylformamide (DMF) and dioxane were gained from Aladdin Reagent Co. Ltd. (Shanghai, China). Ascorbic acid (AA, 99%) and 6-mercapto-1-hexanol (MCH) were got from Sigma-Aldrich (St. Louis, MO, USA). K$_4$Fe(CN)$_6$ and K$_3$Fe(CN)$_6$ were contained in 5 mM [Fe(CN)$_6$]$^{3-/4-}$ solution. 0.1 M Phosphate buffer (PB, pH 7.4) was prepared by the buffer pair of Na$_2$HPO$_4$ and KH$_2$PO$_4$, including 0.1 M KCl as supporting electrolyte. Other reagents used through the whole work were of analytical grade. TE buffer (10 mM Tris-HCl, 1 mM ethylenediaminetetraacetic acid (EDTA), pH 8.0) was used for the storage of all the oligonucleotides. STE buffer (10 mM Tris-HCl, 150 mM NaCl, 1 mM EDTA, pH 8.0) was used as the reaction buffer for the reaction of oligonucleotides. All hairpin DNA were heated at 95 °C for 5 min and then slowly cooled down to 25 °C for annealing before use.

2. Instrumentations

Electrochemical impedance spectroscopy (EIS) was recorded via CHI 604D electrochemistry workstation (Shanghai Chenhua Instrument Co., China). PEC measurements were performed via CHI 440A electrochemical workstation, which was

47 configured with PEAC 200A (Tianjin AiDa Hengsheng Technology Co., Ltd., China)

48 for visible-light excitation. Polyacrylamide gel electrophoresis (PAGE) were carried

49 out on the DYCP-31E electrophoresis apparatus (WoDeLife Sciences Instrument Co.,

50 Ltd., China). A three-electrode system was built for signal collection. To be specific, a

51 modified glassy carbon electrode (GCE, Φ = 4 mm), a platinum wire and an Ag/AgCl

52 (sat. KCl) were employed as the working electrode, the auxiliary electrode and the

53 reference electrode, respectively. The surface morphologies and element components

54 of nanomaterials were recorded by scanning electron microscope (SEM, JSM-7800 F,

55 JEOL Ltd, Tokyo, Japan) coupled with an Oxford-INCA energy dispersive X-ray

56 spectroscopy (EDX). Transmission electron microscopy (TEM, FEI Co., America) was

57 also used to record the appearances of these materials via a Tecnai G2 F20 transmission

58 electron microscope operating at an accelerating voltage of 200 KV (FEI, America).

59 Atomic force microscopy (AFM, Bruker Co. Germany) was utilized to characterize the

60 morphologies and thick of materials. Spectral measurements were performed via

61 Fourier transform infrared spectrometer (FTIR, Nicolet IS10, ThermoFisher Scientific,

62 USA), F7000 fluorescence spectrophotometer (FL, Hitachi High-TechScience Co.,

63 Tokyo, Japan), UV-2600 UV-vis spectrophotometer (UV-Vis, Shimadzu, Japan) and

64 X-ray photoelectron spectrum (XPS) with a VG Scientifc ESCALAB 250 spectrometer

65 (Thermoelectricity Instruments, USA). All the experiments were performed at 25 ± 1

66 °C.

67

3. Synthesis of PTCA

PTCA was synthesized according to previous report[1] with slight modification. First, 51.4 mg PTCDA was dissolved in 20 mL of KOH (5%) under stirring at 65 °C. Later, the reaction solution was cooled down to 25 °C, and HCl (0.9 M) was added dropwise until an orange-red precipitate was observed. Finally, an orange-red precipitate was obtained. The precipitate was centrifuged and collected at 4 °C for future use.
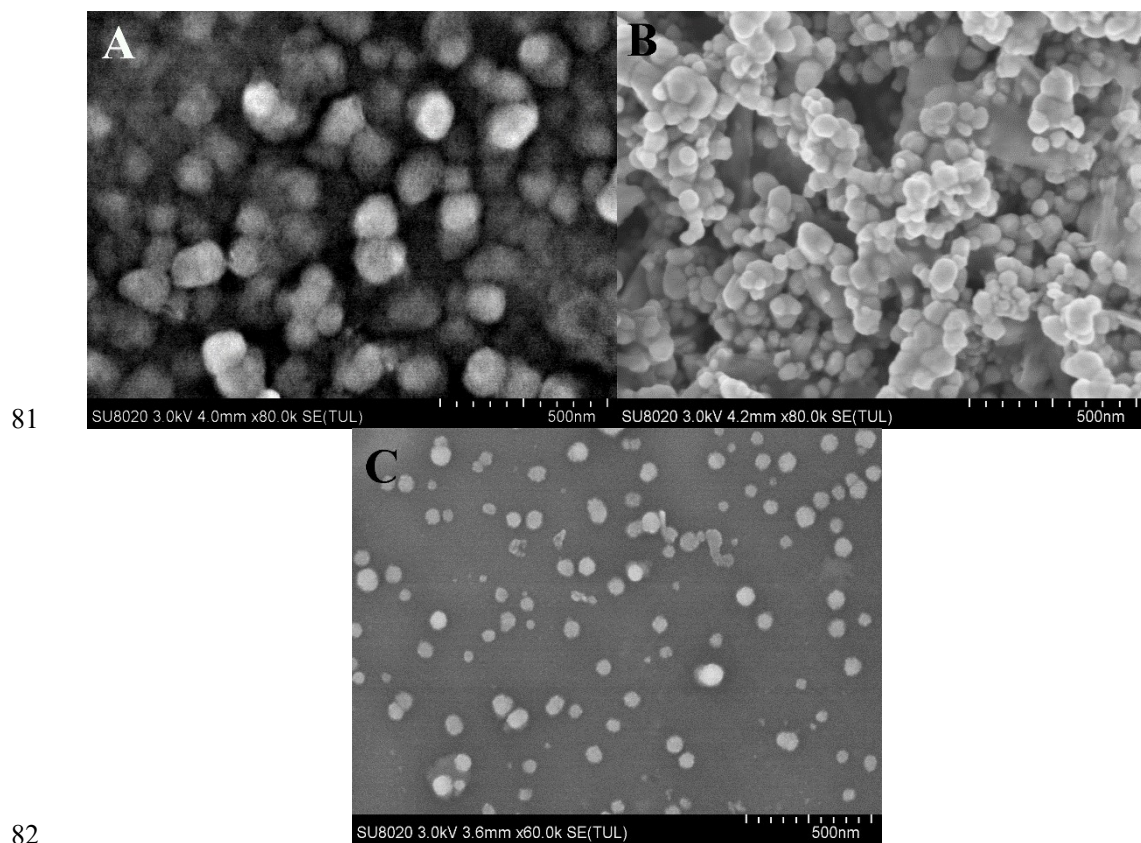
75 **4. SEM images of MBs and MBs-H1**

76
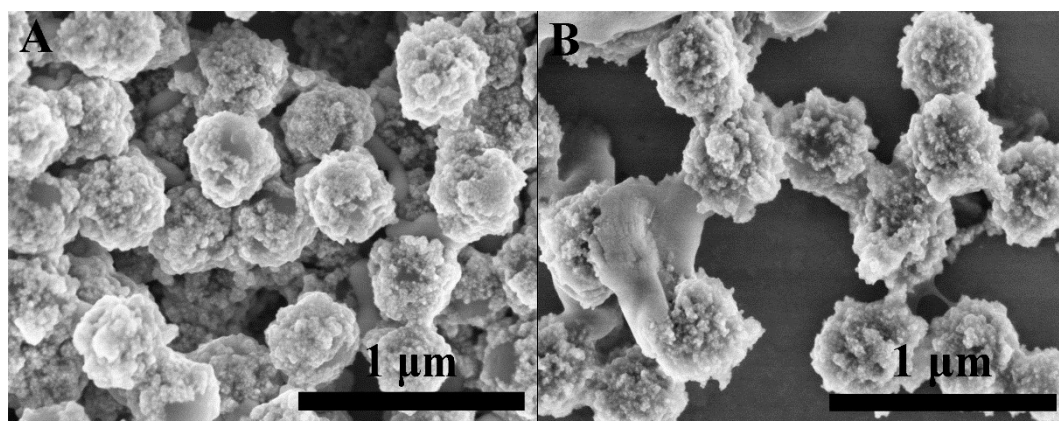
77
78   **Fig. S1.** SEM images of (A) MBs (B) MBs-H1 (insert: partial enlarged image).

79

5. SEM images of ZnO NPs, ZnO NPs-H2 and ZnO NPs-H2-Au NCs

Fig. S2. SEM images of (A) ZnO NPs, (B) the complex of aminated zinc oxide nanoparticles and

carboxyl-hairpin DNA2 (ZnO NPs-H2) and (C) the complex of aminated zinc oxide nanoparticles,

carboxyl-hairpin DNA2 and AS@Au NCs (ZnO NPs - H2 - AS@Au NCs).

6. XPS analysis of PTCA MOFs

Table S1. XPS analysis of PTCA MOFs.

Bonding situation	Binding energy (eV)	Atomic %
C-C (C 1s)	284.73	79.28
C=O (C 1s)	288.48	12.83
π-π (C 1s)	290.05	6.17
C-O (C 1s)	286.60	1.72
O-Mg (O 1s)	531.46	59.72
O-C (O 1s)	533.43	40.28
Mg-O (Mg 1s)	1304.21	100

7. FTIR analysis of PTCA MOFs

Table S2. FTIR analysis of PTCA MOFs.

Wavelength / cm^{-1}	Mode of vibration
3440	stretching vibration of -OH
3120, 3100	stretching vibration of C-H in benzene
1774, 1743	stretching vibration of carbonyl
1594, 1564, 1508, 1461, 1406	skeleton vibration of aromatic ring
1236, 1147, 1121, 1024	stretching vibration of C-O
774	bending vibration of C=O
792, 734	bending vibration of C-H

8. Electrochemical data and calculated energy levels

Table S3. Electrochemical data and calculated energy levels.

| Porphyrins dots	E_{ox} / eV	E_g / eV	E_{HOMO} / eV	E_{LUMO} / eV
PTCA	1.08	1.92	-5.48	-3.56
Mg-PTCA MOFs	1.10	1.50	-5.50	-4.00

9. PEC and Electrochemical responses of the stepwise modified electrodes

The photocurrent changes of different modified electrodes are showed in Fig. S3A. The photocurrent obtained from bared GCE is close to zero (curve a). After modifying the photoelectric material Mg-PTCA MOFs on bared GCE, a much higher photocurrent about 40 μA is gained (curve b). With the reaction between capture DNA and Mg-PTCA MOFs through amide bonds, the decreased PEC signal is observed (curve c). Then the photocurrent further decreases after the incubation of MCH and AS @ Au NCs successively (curve d and e). Finally, with the help of regeneration DNA, the photocurrent is recovered close to the previous step (curve f). Fig. S3B exhibits the EIS behaviors of stepwise modified electrodes. After coating the bared GCE with Mg-PTCA MOFs, the increased charge-transfer resistance (R_{et}) is obtained (curve a and b). With the stepwise modification of capture DNA, MCH and AS @ Au NCs, R_{et} increases sequentially (curve c to e). Along with the incubation of regeneration DNA, R_{et} decreases contributing to the hybrid of regeneration DNA and AS, which makes AS @ Au NCs away from the electrode surface (curve f).

10. Condition optimization

The PEC signals towards 100 fM miRNA 21 in various pH detection solutions are shown in Fig. S3C. The photocurrent decreases with the increase of the pH value until pH 7.4, so pH 7.4 was selected as an optimized value. As illustrated in Fig. S3D, the incubation time of AS@Au NCs was also investigated. The photocurrent drops accordingly with the extension of the incubation time and reaches a platform after 2.0

120 h, so the optimum incubation time of AS@Au NCs is selected as 2.0 h. Furthermore,

121 as shown in Fig. S3E, the PEC signal increases with the increase of the wavelength of

122 the excited light source, while the highest photocurrent is observed with the irradiation

123 of white light. So we choose the white light as the optimal light source throughout the

124 experiment.

125

126

127
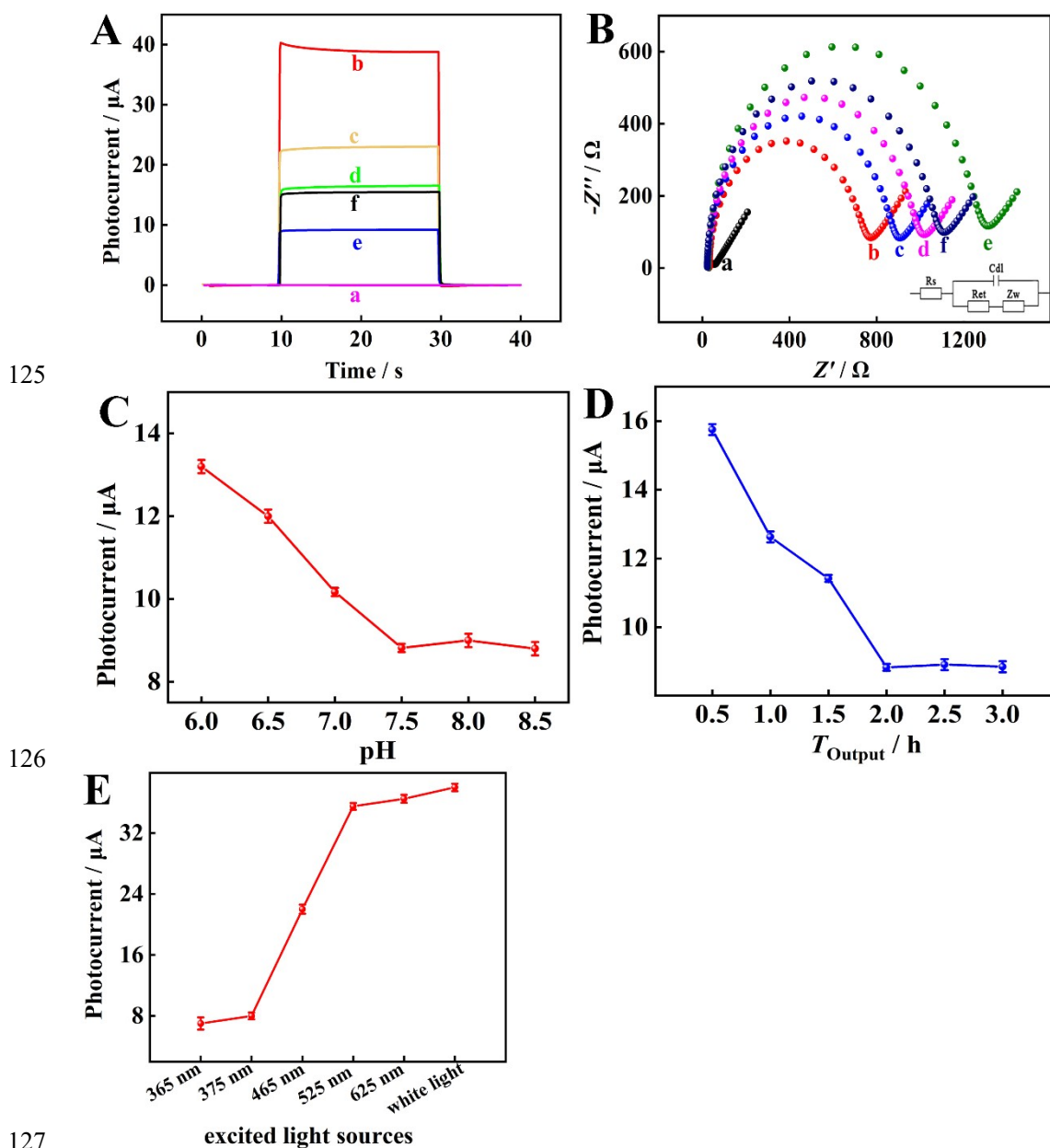
128 **Fig. S3.** (A) PEC responses and (B) EIS profiles (insert: equivalent circuit) of different modified

129 electrodes: (a) bared GCE, (b) Mg-PTCA MOFs / GCE, (c) Capture DNA / Mg-PTCA MOFs / GCE

130   (d) MCH / Capture DNA / Mg-PTCA MOFs / GCE, (e) AS @ Au NCs / MCH / Capture DNA /

131   Mg-PTCA MOFs / GCE, (f) Regeneration DNA / AS @ Au NCs / MCH / Capture DNA / Mg-PTCA

132   MOFs / GCE. The effects of (C) pH, (D) the incubation time of AS@Au NCs and (E) the

133   wavelengths of excitation lights.

134

11. The effect of ZnO NPs and HNO$_3$

In order to investigate the influence of ZnO NPs to the prepared PEC sensing platform, we have designed a contrast experiment by replacing AS@Au NCs (generated by destroying 3D-Sca) by themselves (curve a), AS@Au NCs (curve b) and ZnO NPs - H2 - AS@Au NCs (curve c). As depicted in Fig. S4, the PEC response of the AS@Au NCs is close to the inherently experimental one. However, ZnO NPs - H2 - AS@Au NCs exhibit a much higher PEC signal. The following conclusions can be drawn by the results above. First, ZnO NPs have been almost dissolved and its effect is negligible. Secondly, HNO$_3$ expresses good dissolving capacity to ZnO NPs and does not affect the subsequent detection performance.

In addition, we have investigated the change of pH value after the destroy of 3D-Sca. The pH of 3D-Sca solution is 7.53. After the addition of HNO$_3$, the pH (7.44) is not nearly changed, which is close to the optimal pH of testing solution (pH 7.4). The possible reasons of the almost unchanged pH value may be the low concentration and the small amount of HNO$_3$, and the excellent buffer capacity of PB solution. The results further demonstrate that HNO$_3$ does not affect the subsequent detection.
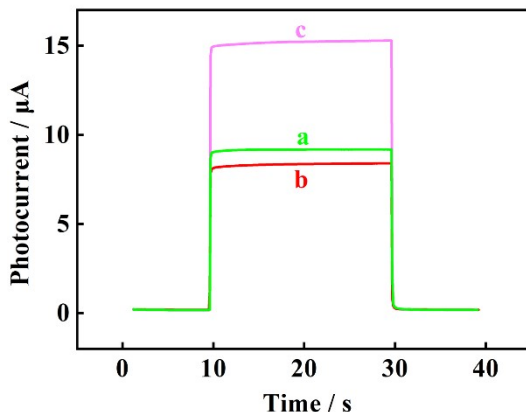
152   **Fig. S4.** The exploration of effect of ZnO NPs and HNO_3 to the proposed biosensor by replacing

153   AS@Au NCs (generated by destroying 3D-Sca) by (a) themselves, (b) AS@Au NCs and (c) ZnO

154   NPs - H2 - AS@Au NCs.

155

156 **12. Comparison with other methods for miRNA 21 detection**

157   **Table S4.** Comparison of the miRNA 21 detection with other detection methodologies.

Analytical method	Detection limit	Linear range	Ref.
CEAM	55 fM	1 pM -10 nM	[2]
SERS	0.34 fM	1.0 fM -10.0 nM	[3]
ECL	0.17 fM	0.5 fM - 10 pM	[4]
SERS	3.5 fM	10 fM - 100 nM	[5]
ECL	0.3 fM	1 fM - 10 pM	[6]
DPV	0.78 fM	10 fM - 1 nM	[7]
DPV	0.434 fM	10 fM - 1000 fM	[8]
PEC	2.8 aM	10 aM - 10 pM	This work

158 **Abbreviations:** cyclic enzymatic amplifcation method (CEAM); surface-enhanced Raman

159 scattering (SERS); electrochemiluminescence (ECL); differential pulse voltammetry (DPV).

160

13. Reference

1. J. Li, W. Tu, H. Li, M. Han, Y. Lan, Z. Dai and J. Bao, *Anal. Chem.*, 2014, **86**, 1306-1312.

2. Q. Li, S. Zhou, T. Zhang, B. Zheng and H. Tang, *Biosens. Bioelectron.*, 2020, **150**, 111866-111874.

3. S. Wen, Y. Su, C. Dai, J. Jia, G.-C. Fan, L.-P. Jiang, R.-B. Song and J.-J. Zhu, *Anal. Chem.*, 2019, **91**, 12298-12306.

4. L. Peng, Y. Yuan, X. Fu, A. Fu, P. Zhang, Y. Chai, X. Gan and R. Yuan, *Anal. Chem.*, 2019, **91**, 3239-3245.

5. J. Chen, Y. Wu, C. Fu, H. Cao, X. Tan, W. Shi and Z. Wu, *Biosens. Bioelectron.*, 2019, **143**, 111619-111626.

6. H. Shao, H. Lin, J. Lu, Y. Hu, S. Wang, Y. Huang and Z. Guo, *Biosens. Bioelectron.*, 2018, **118**, 247-252.

7. S. Su, W. Cao, W. Liu, Z. Lu, D. Zhu, J. Chao, L. Weng, L. Wang, C. Fan and L. Wang, *Biosens. Bioelectron.*, 2017, **94**, 552-559.

8. X. Sun, H. Wang, Y. Jian, F. Lan, L. Zhang, H. Liu, S. Ge and J. Yu, *Biosens. Bioelectron.*, 2018, **105**, 218-225.